Proceedings of GPPS Forum 18
Global Power and Propulsion Society
Zurich, 10th-12th January 2018
www.gpps.global

GPPS-2018-0022

Roughness effects on flow and heat transfer in a ribbed duct considering additive manufacturing

Edward Kilpatrick
Queen's University Belfast
ekilpatrick02@qub.ac.uk
Belfast, United Kingdom

Sung in Kim
Queen's University Belfast
s.kim@qub.ac.uk
Belfast, United Kingdom

ABSTRACT

With the advent of additive manufacturing (AM) and the technological improvements of AM, its potential utilization in gas turbine components manufacturing has been extensively explored nowadays. The AM will increase the turbine design space to develop advanced cooling schemes with improved cooling efficiency. However, the large surface roughness, particularly in small internal geometries, becomes one of key challenges. The effects of surface roughness, inherently caused by AM, on pressure loss and heat transfer are of interest. The thermo-fluidic behaviours in a ribbed duct and the effects of surface roughness on the heat transfer performance are numerically studied using a commercial CFD solver, ANSYS Fluent.

The computational treatments of surface roughness are explored against the experimental results of the additively manufactured channel flows. The appropriateness of the conventional empirical correlations of the equivalent sandgrain roughness height to the arithmetic mean roughness is evaluated in the AM channel flows. A new correlation which best fits the relationship between the arithmetic mean height and sand grain height is proposed to accurately implement the experimental data into simulations.

The accuracy and suitability of the numerical model is validated against the existing experimental results of a stationary duct with square ribs 45 degree angled to the main flow direction. Additional computations are done for the application of different surface roughness representing AM finishing. The influence of the increase in surface roughness are discussed and presented in terms of Nusselt number and skin friction coefficient. The detrimental effect of the surface roughness on the heat transfer performance in a ribbed duct flow is observed.

INTRODUCTION

The gas turbine has a long history and great array of applications in the modern world. In 2011, Mitsubishi Heavy Industries tested the first >60% efficiency gas turbine, an impressive feat, as the importance of gas turbines in generating power for our cities, as well as propulsion for aeronautical applications is substantial. A large factor in increasing the efficiency of a gas turbine is the turbine inlet temperature and the maximum possible temperature that the turbine blades are capable of withstanding without failure due to modes such as creep. Creep becomes more significant under high temperatures. It creates a limit on the maximum allowable turbine inlet temperature and, therefore, also creates a limit on the efficiency that can be yielded from gas turbines. The differential between the temperatures the blades can withstand and the temperatures the blades are exposed to must be addressed through the employment of turbine cooling techniques. One of such cooling techniques, which is explored further in this study, is the employment of internal ducts through which cool air is passed and the blade temperature reduced. It is clear, therefore, that the enhancement of the efficiency of cooling the turbine blade can directly lead to an increase in turbine inlet temperature and an improvement in the efficiency of the gas turbine engine. To do this, ribs are introduced into the duct, disrupting the formation of the attached boundary layer and increasing the heat transfer along all surfaces exposed to the fluid.

In addition, manufacturing techniques can also have an important bearing on the ability of cooling schemes to disperse heat more efficiently. A relatively recently introduced technique, first developed in 1981 by Hideo Kodama of Nagoya Municipal Industrial Research Institute, additive manufacturing is regarded as the future of manufacturing. Also, it may herald significant advances in the production of gas turbine blades. However, the inherent surface roughness of additively manufactured parts, is generally considered as a significant shortcoming of the technique. Therefore, the effect of the surface roughness on flow and heat transfer needs to be investigated carefully and it is the main parameter of this numerical study. The surface roughness is typically experimentally measured in a different format from the way of implementation in CFD simulations.

There are many relationships between these two values presented for a variety of different 'rough' surfaces. It is, therefore, important that significant reviewing of literature and testing of these relationships is undertaken to correctly apply the roughness into the CFD model, in order to investigate the effect of surface roughness on fluid behaviour and heat transfer performance of the cooling channel.

The Flow and Heat Transfer in a Ribbed Duct

The rib turbulators are introduced to create an area of flow separation, disrupting the formation of the attached boundary layer and promoting turbulent conditions in the duct. Early experiments, including Burggraf (1970), Han et al. (1978) and Han (1984), considering rib turbulators regularly spaced, positioned on two opposite walls of the duct and measuring their effect on heat transfer found the following parameters to be of particular importance;

Rib pitch-to-height ratio – P/e
Rib height-to-hydraulic diameter ratio e/D_h
The Aspect ratio of the rectangular channel, AR
This is defined as the ratio between the width, W, of the ribbed side and the channel height, H

A turbulent flow regime with minimal or no attached boundary layer formation are the optimum conditions in maximising heat transfer and so the various considerations for a rib as listed above play a large role in the effectiveness of the turbulators in increasing heat transfer. Besides these, the most critical factors in the enhancement of heat transfer are the angle of the rib relative to the mean flow direction, or the angle-of-attack, and the spacing between the ribs as these factors hugely affect the flow patterns in the duct.

Tanda (2011) used an electric heater with a constant heat flux to investigate the effect of rib spacing, in the form of a ratio of rib spacing to rib height p/e, on heat transfer and friction at a constant rib angle of 45° normal to the flow of fluid and varying number of ribbed walls (one or two). He noted that heat transfer was enhanced by three-dimensional flow patterns generated through the interaction of oblique secondary flows with the main flow over the ribbed wall and put particular emphasis on how the secondary flow moves along the rib profile, away from the upstream acute angled-rib side of the channel before turning back on itself and carrying cold fluid from the core region towards the ribbed surface located near the acute side. In a simulation investigating various angles and pitch to height ratios for a coolant channel with two ribbed walls conducted by Kim et al. (2009), they noted that for angles lower than 40° or higher than 70°, the intensity of the swirling flow, that is the flow that moves along the angled rib, becomes weak but for angles between 40° and 70°, the flow intensity is strong. It is between this range that the specified angle should lie.

Other rib shapes have also been considered and, in an experiment conducted by Olsson and Sunden (1998), the standard arrangement of parallel ribs are compared against V shaped ribs facing in two directions. While parallel V shaped ribs pointing opposite the direction of flow yields the highest results for heat transfer, generation of the geometry is difficult and the difference between V shaped ribs and normal parallel ribs is not enough to warrant the extra effort required. Additive Manufacturing techniques, however, could generate these geometries with relative ease. In two almost identical experiments conducted separately by Bonhoff et al. (1999) and Chanteloup et al. (2002), a wealth of data were presented for geometries which give rise to high intensity vortices and eddies and large heat transfer coefficient. This geometry was selected for this study.

Additive Manufacturing

Additive manufacturing (AM) is increasingly becoming a relevant manufacturing technique due to ever progressing technological advances. Particularly, direct metal laser sintering (DMLS) has a lot of potential in the production of gas turbine components as this method broadens the design space as well as permitting the design and generation of far smaller and more complex geometries than were previously available from more traditional manufacturing techniques at a moderate monetary cost.

However, in comparison to more traditional manufacturing techniques, the surface roughness generated with AM can be substantially larger. Typically, this roughness would be removed with various roughness removal technologies but these technologies are also limited in that they cannot smooth the surfaces of small tortuous channels such as that which would be encountered in gas turbine components.

Scaling Roughness Effect in Simulation

Many of the experimental studies involving roughness effects on thermal performance, and more importantly the studies which will be replicated in this report, quantify roughness with the arithmetic average height, R_a. However, in CFD simulation, the typical value used to describe roughness is the sand grain height, k_s. Therefore, one of the main problems when applying roughness to a simulation is finding an appropriate relationship which can bridge the two different values, R_a and k_s, in an accurate manner with considering the manufacturing technique used to generate geometry. To date, a wide variety of relationships have been proposed and Boyle and Senyitko (2003) showed that estimated values for k_s can vary up to an order of magnitude depending on the roughness characterization. In the experiments (Stimpson et al., 2016), the arithmetic average height, R_a, was largely found to lie within the range of 6 µm – 20 µm with the occasional outliers and thus, the surfaces of roughness within this range were considered when comparing the relationships between R_a and k_s. Additionally, due to a lack of literature pertaining to sand grain roughness of Additively Manufactured products, correlations for differently manufactured surfaces of a similar roughness scale were compared.

According to a manufacturer (FineTubes, 2017) of metal tubing for a range of applications, the method of forging

produces an arithmetic average surface roughness range of 3.2 µm - 12.5 µm which falls in same order of magnitude of roughness for AM parts. In order to link these values to the sand grain roughness height, Schaffler (1980) specified the following relationship for forged and machined blades;

$$k_s \approx 8.9R_a$$

This relationship was developed by measuring the blade surface roughness of a large variety of forged and electrochemically machined blades with a roughness measurement device called a Perthometer. He suggested that because the arithmetic mean height of the roughness elements included a large portion of far smaller elements, which are fully submerged in the laminar sub layer and therefore not at all felt by the turbulent flow, as well as the larger roughness elements which actually affected flow characteristics, the value R_a would not be useful in determining the hydrodynamic characteristic of the surface. The value of k_s that they proposed was therefore determined by analysing the peaks and was defined as '*the difference between the arithmetic averages of the ten highest peaks and the ten deepest grooves which exist per millimetre length'*.

Bammert and Sandstede (1976) proposed a relationship for mechanically produced surfaces and emery grain surfaces, in accordance with their own measurements for emery grain surfaces, which is as follows;

$$k_s \approx 2.2R_a^{0.88} \quad (1)$$

Such surfaces can have a large range of roughness, R_a, spanning from 0.1 µm – 100 µm.

Finally, in a follow up paper, Stimpson et al. (2017) proposed a relationship between R_a and k_s by linking the hydraulic diameter D_h and found that it provided the best correlation for fully turbulent flow, despite being among the simplest statistical measures. The expression is shown below.

$$\frac{k_s}{D_h} = 18\frac{Ra}{D_h} - 0.05 \quad (2)$$

Despite the wealth of available relationships between k_s and R_a, the relatively new technique of AM and the untested geometry on which it shall be applied may prove incompatible upon commencement of the simulations with the above equations and require a new, unique correlation.

ANSYS Fluent also presents a roughness constant input, C, which can be used to describe the uniformity of the roughness (ANSYS, 2017). The default value given, C=0.5 (indicating the uniform distribution of the roughness on the surface), reproduces Nikuradse's resistance data for pipes roughened with tightly-packed, uniform sand-grain roughness (Nikuradse, 1950). Where the roughness to be generated begins to depart from uniformity, a higher value of C is required up to a maximum value of C=1.0. A value of C=0.5, indicating uniformity in the roughness, was used for the present simulations of the experimental cases of Additively Manufactured channels and its implementation into the ribbed cooling duct.

Computational Model of AM Channel

In order to appropriately apply the surface roughness of additive manufacturing to the cooling channel flow simulation, the validation of CFD model and the evaluation of roughness correlations were firstly performed against the experiments of the additively manufactured channel flows (Stimpson et al., 2016). In the experiments, five rectangular channels were manufactured using DMLS with a material, a powered cobalt-chrome-molybdenum-based superalloy (CoCr). Three channels among those were recreated in CFD models using a commercial CFD package, ANSYS Fluent R17. The dimensions and corresponding roughness of each case are as follows shown in Table 1.

The simulations were run for an inlet Reynolds number varying from 3,000 to 10,000 at room temperature. All AM channel simulations were run with a wall heating condition, a constant wall heat flux of 50,000 W/m^2 and only a half of the channel was simulated with a symmetry plane along the lower surface of the computational domain. For the turbulence closure, the k-ω SST model was selected. The residuals met convergence criteria of 1E-5. Initially, a grid convergence study was conducted for a refinement factor of 2 and the simulations were deemed suitably converged to warrant further simulations. The y+ of the cases of the grid study also met the requirements of the k-ω SST model of 1. The finally selected mesh has a total of 499,200 elements.

Table 1 – Dimensions and Roughness of the AM channels (Stimpson et al., 2016)

Coupon	Design Width (µm)	Design Height (µm)	Design D_h (µm)	R_a, Area Weighted Average (µm)
M-1x-Co	305	660	406	10.3
M-2x-Co	610	1321	834	12.7
S-2x-Co	610	610	610	9.5

Table 2 – A comparison of Nusselt number between simulated and empirical values for M-1x-Co

Reynolds Number	Simulated Nusselt Number	Gnielinski Nusselt Number
3625	12.59	11.98
4810	15.55	15.88
6420	19.04	20.66

Validation of AM channel flow

First, smooth channel flows were simulated and the Nusselt numbers were compared against the empirical Gnielinski correlation (Incropera and DeWitt, 2006), which is shown in Equation (4).

$$Nu = \frac{\frac{f}{8}\times(Re-1000)Pr}{1+12.7\sqrt{(\frac{f}{8})}(Pr^{\frac{2}{3}}-1)} \quad (4)$$

The Gnielinski correlation, which is valid for a range of 3,000 ≤ Re ≤ 5,000,000, was selected for comparison as opposed to the Dittus–Boelter equation which would not produce accurate results for the selected range of Reynolds number. The simulations showed good agreement with the Gnielinski correlation and Table 2 displays the agreement between simulated and empirical values.

Table 3 – Comparison of Nusselt numbers between different roughness correlations for M-1x-Co

Reynolds number	3625	4810	6420
Stimpson et al. (2017); $18R_a/D_h - 0.05$	46.2	59.6	69.7
Bammert & Sandstede (1976); $2.2R_a^{0.88}$	31.2	48.8	60.1
Schaffler (1980); $8.9R_a$	33.2	51.4	67.3
Experimental measurements (Stimpson et al. 2016)	30.6 – 33.1	42.4 – 45.5	55.7 – 59.8

The reviewed relationships between k_s and R_a were tested against the experiment of AM channels and summarized in Table 3. It was found that the relationship proposed by Stimpson et al. (2017) resulted in a Nusselt number far above the experimental data, while the Bammert and Sandstede correlation was far better suiting for the M-1x-Co coupon (R_a = 10.3 μm). When this was then applied to other coupons however, the correlation proved to be less successful. Schaffler's correlation was then employed which yielded still inaccurate results, albeit closer and linearly offset from the required data. Following the employment of these correlations, it was deemed necessary to propose a new relationship for the simulation of roughness of additive manufacturing using ANSYS Fluent and the newly modified relationship is presented in Equation (6):

$$k_s = 8R_a \quad (6)$$

This relationship was heavily influenced by Schaffler's data with only a slight adjustment made to the constant which represents the enhancement of the arithmetic mean height of the roughness elements so as to only represent the roughness which influences the flow characteristics. As the products of Additively Manufactured components receive a similar, although slightly offset, inherent roughness as those manufactured by forged parts, this is a reasonable modification to make.

The comparison of the Nusselt number against the experimental data (Stimpson et al., 2016) is presented in Figure 1 for all roughness relationships on the coupon M-1x-Co (R_a = 10.3 μm), including the proposed roughness correlation. As shown in Figure 1, the newly proposed correlation showed the best agreement with the experimental data. The proposed correlation was then compared against the different roughness of the other coupons, M-2x-Co (R_a = 12.7 μm) and S-2X-Co (R_a = 9.5 μm). The result of these further simulations served to validate the accuracy of this correlation when being applied to the additively manufactured channel flows. The data is presented on a log scale graph and compared against the measured data in Figure 2. Additionally, the arithmetic mean roughness height and the corresponding sand-grain roughness height adhering to the proposed relationship can be found in Table 4 for the three coupons simulated.

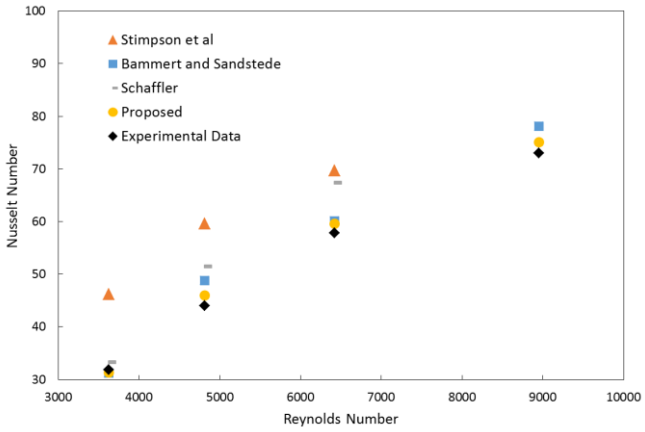

Figure 1 - Comparison of the reviewed and proposed correlations against the experimental data (Stimpson et al., 2016)

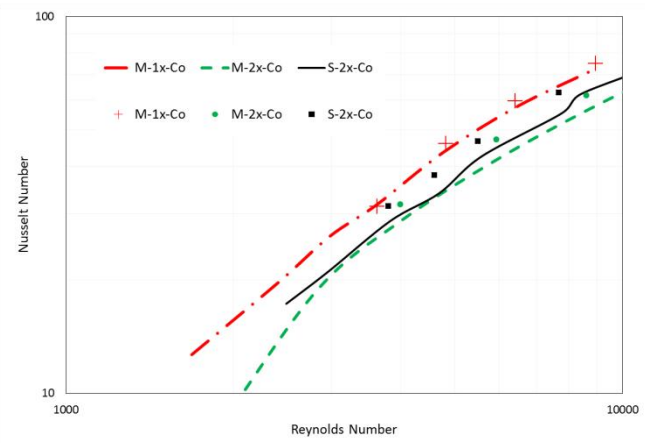

Figure 2 – Comparison of experimental and simulated results (Line represents experimental data and point represents simulated data)

Table 4 – Sand-grain roughness for simulated coupons from the proposed correlation

	R_a	k_s
M-1x-Co	1.03E-05	8.240E-05
M-2x-Co	1.27E-05	1.016E-04
S-2x-Co	9.50E-06	7.600E-05

As can be observed in comparing the data from the simulations with the experimental data in Figure 2, the roughness effects of the various simulated coupons reflects well the trend of Nusselt number in the equivalent coupons of their experiments. The data presented also serves to confirm that a relationship between the measured arithmetic average roughness height and the equivalent sand grain roughness value used in simulations has been successfully found and validated against the experimental data.

SIMULATION OF A RIBBED COOLING CHANNEL FLOW

Computational model of a ribbed cooling channel

A ribbed cooling channel flow was simulated to consider the effect of the surface roughness of additive manufacturing. The geometry and mesh were imported from the former work (Kim and O'Sullivan, 2016). The computational domain was built based on the experimental works (Bonhoff et al., 1999 and Chanteloups et al., 2002); The channel height-to-width aspect ratio is one with the hydraulic diameter (D_h) of the channel is 100 mm. The rib pitch to rib height ratio (P/e) is 10. The rib height to hydraulic diameter ratio (e/D_h) is 0.1. The computational domain also included a 600 mm inlet section which allows the flow to fully develop before encountering the ribs, 6 ribs to allow the flow to develop but not needlessly expend computational resources, and an outlet section of two and a half rib pitches to prevent the outlet from influencing the results of the test section. Figure 3 shows the computational domain of the half of a ribbed duct with a upper symmetric plane. At the inlet, the velocity of the air was specified at 7.82 m/s in order to give a Reynolds number of 50,000 based on the hydraulic diameter. The convergence was determined through the use of monitors which were set on the various components of velocity at a distinct point as well as the mass flow rate at the outlet plane. The computational domain contained 6.6 million elements. This fine mesh used had already been subjected to the previous grid convergence analysis (Kim and O'Sullivan, 2016) and so it may be assumed that the results are not at risk of discretization error.

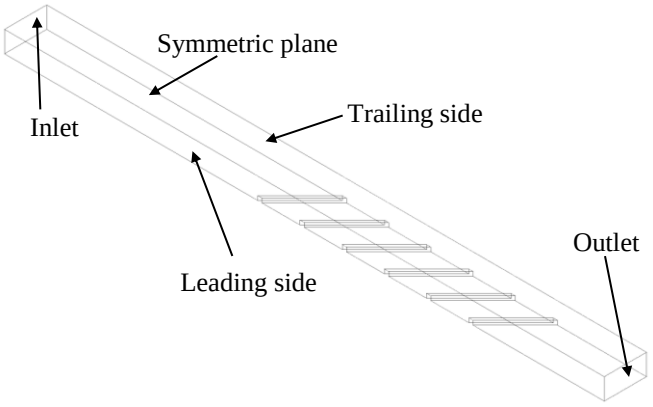

Figure 3 – Computational domain of a Ribbed Duct

The effect of roughness in a ribbed cooling channel flow

Simulations were carried out in order to investigate the effect of the surface roughness on the flow and heat transfer characteristics in a ribbed cooling channel. The surface roughness in additive manufacturing is affected by the surface orientation of manufacturing, up to several times difference between the minimum and the maximum surface roughness (Snyder et al., 2016). In this context, the typical range of AM surface roughness, around R_a = 10 μm to 100 μm, was considered. From the numerical test, the area-averaged Nusselt number (Nu) on only the inter-ribs surface was computed and listed in Table 5. Nusselt numbers from the experiment (Chanteloup et al., 2002) and the smooth surface case were also provided for the comparison. Nusselt number was normalized by using the Dittus-Boelter equation (Incropera and DeWitt, 2006) for a smooth duct flow without ribs. It is as follows;

$$Nu_0 = 0.023 \times Re^{0.8} Pr^n$$

where n=0.4 for fluid in a heating condition.

Additionally, the area-averaged skin friction coefficient (C_f) on the inter-ribs surface was also compared to determine whether the hydraulic performance would be adversely affected by the introduction of Additive Manufacturing.

Table 5 – Comparison of Nusselt number and friction coefficient with varying surface roughness

Roughness	Nu / Nu_0		C_f	
Exp. (Chanteloup et al. 2002)	2.78	–		
R_a = 0 (Smooth)	2.94	5.8%	0.0222	–
R_a = 10.3 μm	2.66	–4.3%	0.0216	–2.7%
R_a = 20.6 μm	2.49	–10.4%	0.0224	1.3%
R_a = 30.9 μm	2.51	–9.7%	0.0241	8.8%
R_a = 51.5 μm	2.58	–7.2%	0.0271	22.4%
R_a = 103 μm	2.63	–5.4%	0.0309	39.5%

In Table 5, the Nusselt number and percentage discrepancy for each increasingly rough case are presented. Heat transfer decreases initially and then increases again as the surface roughness, R_a, increases. Contrary to the former validation cases of the micro channels, the Nusselt numbers of all the rough surface cases of the ribbed duct flow are reduced from the case of smooth surface, but not significant. However, the results show a significant increase in the skin friction coefficient, C_f, with the surface roughness increase. In the present case, the effect of roughness on the skin friction is more significant than on the heat transfer. It is attributed to the different scale of the channels and the different flow structures between the micro channel and the ribbed duct. The ratio of the roughness to the hydraulic diameter (R_a/D_h) of this ribbed duct case is around 0.001, which is much smaller than that of the micro channel cases (R_a/D_h = 0.1 – 0.2). The vortical flow structures caused by the ribs are dominant in the ribbed duct flows, whereas the turbulent boundary layer has the main role in the flow and heat transfer of the micro channel. The details of the effect of

the surface roughness on the flow and heat transfer in the ribbed duct are to be discussed in the following section. When comparing the cases with increasing roughness, (from R_a = 10.3 μm to R_a = 103 μm), it is also clear that the relationships of Nusselt number and skin friction against the surface roughness is non-linear. This is an area that requires further investigation to determine the most effective roughness case in terms of heat transfer efficiency as well as pressure drop. Additionally, the use of AM for the manufacture of turbine blades and the internal coolant channels would not be viable if the hydraulic performance of the new components were not as high as would be produced through previous manufacturing techniques. For this reason, the large increase of the skin friction coefficient and the decrease of Nusselt number in the present cases becomes one of critical challenging points that AM has to overcome.

The effect of roughness on the vortical flows and heat transfer in a ribbed duct

In this kind of ribbed duct flows, the vortical flows caused by the inclined rib are dominant flow structures and taking a dominant role in the heat transfer enhancement (Bonhoff et al., 1999; Chanteloup et al., 2002; Kim and O'Sullivan, 2016). The vortical flow structures over the inclined rib can be seen in Figure 4, the vorticity contour plots. The main duct flow separates from the wall in front of the rib. The detached shear layer goes over the rib and generates a large vortical flow structure downstream of the rib. Due to the inclination of the rib, the relatively smaller and stronger vortical structure is generated near one side wall (a leading side where the main duct flow encounters the inclined rib, first) and then it is growing up along the inclined rib from the leading side to the other (a trailing side where the duct flow meets the rib later). The larger vortical flow impinges to the other side wall (the trailing side) at the end.

For all three cases of smooth surface and two different roughness, the same vortical structures can be seen in Figure 4. However, the strength of the vortex for the rough surface cases is weaker than that of the vortex in the smooth surface case. The shape of the vortex in the smooth surface case is circular, whereas the vortex is stretched to elliptical shape with the increase of the surface roughness. Eventually, the rough surface makes the vortical flow weaker in the ribbed duct.

In order to see the relation between the surface roughness and the flow behaviour, the skin friction distribution is compared in Figure 5. With increasing the surface roughness, the higher skin friction coefficient distribution on the larger area can be seen in Figure 5. The increased surface friction due to the increased roughness results in the adverse effect on the development of the large vortical flow structures in the inter-ribs region.

From the experimental observations (Bonhoff et al., 1999; Chanteloup et al., 2002) and the present simulation of the smooth wall case, the maximum heat transfer region is found to be just beneath of the vortical flow structure rather than the region of the re-attachment of the shear layer. The stronger vortex and faster recirculating flows enhance the heat transfer performance in this case. However, the rough surface makes the vortical structure weaker. As a result, the heat transfer is decreased. It is confirmed in the normalized Nusselt number (Nu/Nu_0) distributions on the ribbed surface shown in Figure 6. For the smooth surface case, the higher heat transfer region downstream of the rib, underneath of the vortical flow, is clear. However, the higher heat transfer region is getting widened and the peak value is getting lower as the surface roughness increases. It is consistent to the variation of the vortical flow structure in Figure 4.

The effect of the surface roughness can be clearly seen in the local velocity profiles in Figure 7. The velocity profiles of the present steady simulations are also compared to the experimental measurements (Chanteloup et al., 2002). The velocity profiles in the central plane of the duct and at the middle point between the fifth and sixth ribs are plotted against the normalized channel height. As the roughness increases, the streamwise velocity (u-velocity) near the wall decreases, but the downwash (negative v-velocity) increases. Conclusively, in a ribbed cooling channel flow where the larger vortical flow structure is dominant, the surface roughness has the detrimental effect on the vortical flows as well as heat transfer performance, consequently.

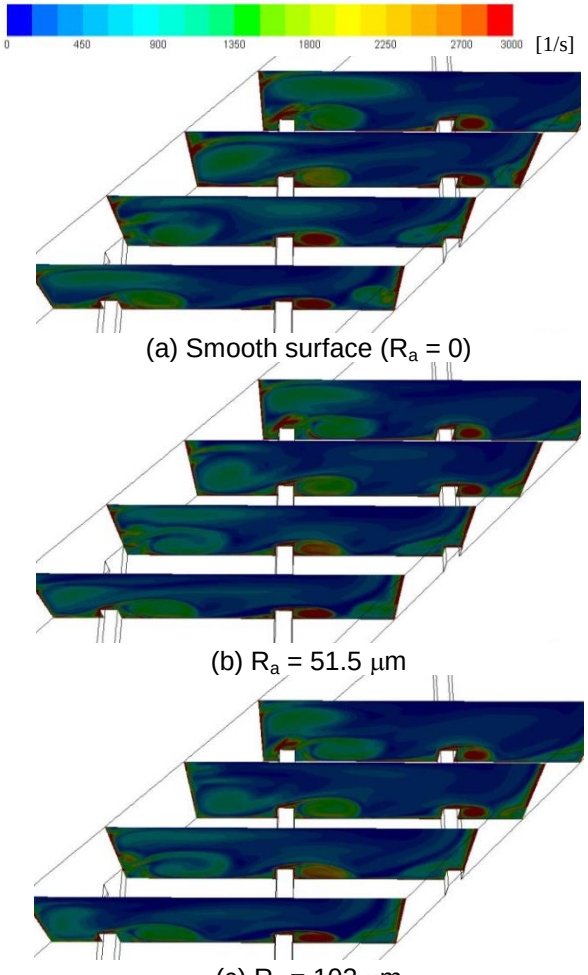

(a) Smooth surface (R_a = 0)

(b) R_a = 51.5 μm

(c) R_a = 103 μm

Figure 4 – Vorticity contours to compare the vortical flows in the ribbed duct

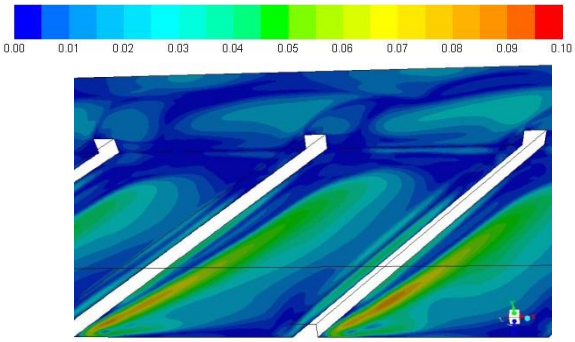

(a) Smooth surface (R_a = 0)

(b) R_a = 51.5 μm

(c) R_a = 103 μm

Figure 5 – Skin friction coefficient distribution with the surface roughness variation

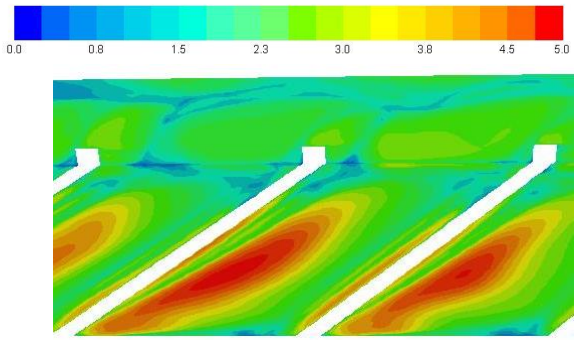

(a) Smooth surface (R_a = 0)

(b) R_a = 51.5 μm

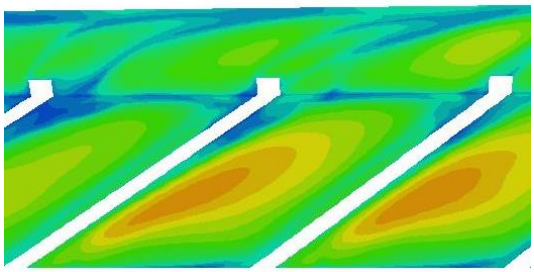

(c) R_a = 103 μm

Figure 6 – Nusselt number (Nu/Nu_0) distribution with the surface roughness variation

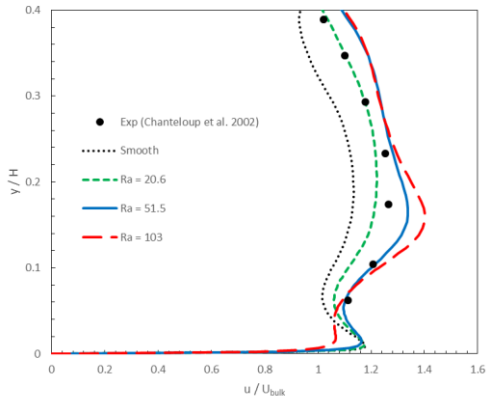

(a) u-velocity

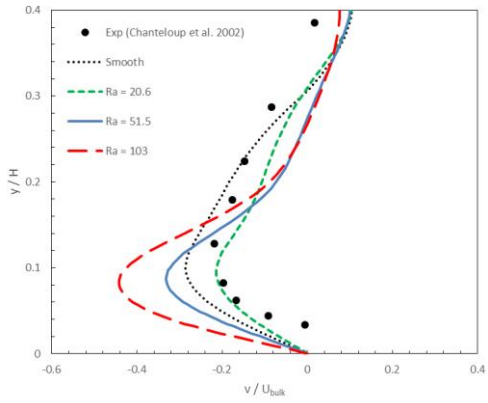

(b) v-velocity

Figure 7 – Comparison of the velocity profiles in the center plane of the duct and at the mid point between 5th and 6th ribs

The prospect of simultaneously increased ease of manufacturing turbine blades and increased efficiency of the coolant channels in distributing heat from the blades presents many possibilities for additive manufacturing and its application within the industry in the future. Further studies in this area, however, are needed to address the following, lingering uncertainties;

1. To more accurately understand the full effect that surface roughness may have on actual ribbed, internal cooling channels of turbine blades, simulations should be run on actual geometries with wide range of scale and operating conditions.

2. Additively manufactured components are susceptible to varying roughness depending on the orientation of the surface generated with downward facing walls typically exhibiting roughnesses up to twice the size of upward facing or vertical walls. This effect should be considered as the uniform roughness was applied to all the surfaces in the present study.
3. Despite good agreement between simulated results and experimental data for the additively manufactured channel, the application of roughness to the CFD model requires additional carefulness, such as y+ variation; in a ribbed duct flow, the average y+ = 5 for smooth surface case and the average y+ = 31 for R_a = 103 μm case.

CONCLUSION

The advent of Additive Manufacturing and the appropriateness of its application into the industry of gas turbine manufacture has been investigated by applying the inherent roughness associated with AM products to the internal cooling channel of a gas turbine blade in terms of heat transfer performance and friction losses. The best fitting new correlation between sand-grain roughness, to be directly input into simulations, and arithmetic mean roughness height, as presented in experimental testing of AM channels, has been determined through the simulations on one coupon, then validated against two additional simulations for coupons of different roughness and compared against heat transfer data presented by Stimpson et al. (2016). The validated roughness correlation was then applied to an internal ribbed duct flow for a gas turbine blade cooling. These simulations have yielded the following results:

- The simulation of AM channel flow was successfully validated and the new proposed correlation of the roughness scaling showed good agreement with AM channel data
- Applying values of roughness typically inherent with additively manufactured parts to the surface of a ribbed duct has been shown to have detrimental effect on the heat transfer efficiency of the cooling channel due to the adverse effect on the large vortical flow structure.
- The increase in friction factor across the increase in surface roughness was significant.
- It is recommended that the surface roughness must be one of the key parameters in the design and development of advanced turbine cooling systems using Additive Manufacturing.

REFERENCES

Bammert, K. and Sandstede, H., "Influence of manufacturing tolerances and surface roughness of blades on the performance of turbines," Journal of Engineering Power, 98(1), pp. 29-36, 1976.

Bonhoff, B., Parneix, S., Leusch, J., Johnson, B. V., Schabacker, J. and Bolcs, A., "Experimental and numerical study of developed flow and heat transfer in coolant channels with 45 degree ribs," International Journal of Heat and Fluid Flow, 20(3), pp. 311-319, 1999.

Boyle, R. J. and Senyitko, R. G., "Measurements and predictions of surface roughness effects on turbine vane aerodynamics," ASME Paper GT-2003-38580, 2003.

Burggraf, F., "Experimental heat transfer and pressure drop with two-dimensional turbulence promoter applied to two opposite walls of a square tube," Augmentation of Convective Heat and Mass Transfer, ASME, pp. 70-79, 1970.

Chanteloup, D., Juaneda, Y., and Bolcs, A., "Combined 3-D flow and heat transfer measurements in a 2-pass internal coolant passage of gas turbine airfoils," Journal of Turbomachinery, 124(4), p. 710-718, 2002.

FineTubes, Surface Finishes. www.finetubes.co.uk/products/technical-reference-library/tube-surface-finishes/ (Accessed 6 July 2017)

Han, J. C., Glicksman, L. R. and Rohsenow, W. M., "An investigation of heat transfer and friction for rib-roughened surfaces," Int. J. Heat Mass Transfer, 21, pp. 1143-1156, 1978.

Han, J. C., "Heat transfer and friction in channels with two opposite rib-roughened walls," J. Heat Transfer, pp. 774-781, 1984.

Incropera, F. P. and DeWitt, D. P., Fundamentals of Heat and Mass Transfer, 6th Edition, John Wiley & Sons, 2006.

Kim, K. M., Lee, H., Kim, B. S., Shin, S. Lee, D. H. and Cho, H. H., "Optimal design of angled rib turbulators in a cooling channel," Heat Mass Trans., 45, pp.1617-1625, 2009.

Kim, S and O'Sullivan, A., "Comparison of hybrid RANS-LES simulations of turbulent flow and heat transfer in a ribbed duct," 6th Symposium on Hybrid RANS-LES Methods, Strasbourg, French, 26-28 Sept 2016.

Nikuradse, J., "Laws of flow in rough pipes," NACA-TM-1292, 1950.

Olsson, C. and Sunden B., "Experimental study of flow and heat transfer in rib-roughened rectangular channels," Experimental Thermal and Fluid Sci., 16, pp. 349-365, 1998.

Schaffler, A., "Experimental and analytical investigation of the effects of Reynolds number and blade surface roughness on multistage axial flow compressors," J. Eng. Power, 102(1), pp. 5-12, 1980.

Snyder, J. C., Stimpson, C. K., Thole, K. A. and Mongillo, D., "Build direction effects on additively manufactured channels," Journal of Turbomachinery, 138, 051006 (8 pages), 2016.

Stimpson, C. K., Snyder, J. C., Thole, K. A. and Mongillo, D., "Roughness effects on flow and heat transfer for additively manufactured channels," Journal of Turbomachinery, 138, 051008 (10 pages), 2016.

Stimpson, C. K., Snyder, J. C., Thole, K. A. and Mongillo, D., "Scaling roughness effects on pressure loss and heat transfer of additively manufactured channels," Journal of Turbomachinery, 139, 021003 (10 pages), 2017.

Tanda, G., "Effect of rib spacing on heat transfer and friction in a rectangular channel with 45° angled rib turbulators on one/two walls," Int. J. of Heat and Mass Transfer, 54(5-6), pp. 1081-1090, 2011.